Research paper

New HSF1 inducer as a therapeutic agent in a rodent model of Parkinson's disease

Irina V. Ekimova[a], Daria V. Plaksina[a], Yuri F. Pastukhov[a], Ksenia V. Lapshina[a],
Vladimir F. Lazarev[b], Elena R. Mikhaylova[b], Sergey G. Polonik[c], Bibhusita Pani[d],
Boris A. Margulis[b], Irina V. Guzhova[b,*], Evgeny Nudler[d,e,*]

[a] Laboratory of Comparative Thermophysiology, I.M. Sechenov Institute of Evolutionary Physiology and Biochemistry of Russian Academy of Sciences, pr. Maurice Thorez, 44, St. Petersburg 194223, Russia
[b] Cell Protection Mechanisms Laboratory, Institute of Cytology Russian of Academy of Sciences, Tikhoretsky pr., 4, St. Petersburg 194064, Russia
[c] G.B.Elyakov Pacific Institute of Bioorganic Chemistry of Far East Branch of Russian Academy of Sciences, pr. 100 let Vladivostoku 159, Vladivostok 690022, Russia
[d] Department of Biochemistry and Molecular Pharmacology, New York University School of Medicine NY, NY 10016, USA
[e] Howard Hughes Medical Institute, New York University School of Medicine NY, NY 10016, USA

ARTICLE INFO

ABSTRACT

Molecular chaperone HSP70 (HSPA1A) has therapeutic potential in conformational neurological diseases. Here we evaluate the neuroprotective function of the chaperone in a rat model of Parkinson's disease (PD). We show that the knock-down of HSP70 (HSPA1A) in dopaminergic neurons of the Substantia nigra causes an almost 2-fold increase in neuronal death and multiple motor disturbances in animals. Conversely, pharmacological activation of HSF1 transcription factor and enhanced expression of inducible HSP70 with the echinochrome derivative, U-133, reverses the process of neurodegeneration, as evidenced by a increase in the number of tyrosine hydroxylase-containing neurons, and prevents the motor disturbances that are typical of the clinical stage of the disease. The neuroprotective effect caused by the elevation of HSP70 in nigral neurons is due to the ability of the chaperone to prevent α-synuclein aggregation and microglia activation. Our findings support the therapeutic relevance of HSP70 induction for the prevention and/or deceleration of PD-like neurodegeneration.

1. Introduction

Parkinson's disease (PD) is a chronic disorder characterized by cardinal motor symptoms and a wide range of non-motor symptoms. PD is currently incurable, and the limited available clinical interventions merely provide symptomatic relief. About 16 million people worldwide suffer from PD, and the incidence rate increases with age. About 1% of PD patients succumb by the age of 65, and 5% succumb by the age of 85 (De Lau and Breteler, 2006). The increase in centenarians predicted over the next 20–30 years will be accompanied by a 1.5–2-fold increase in PD patients (Dorsey et al., 2007).

The pathologic features of PD include the loss of dopaminergic (DA) neurons in the substantia nigra pars compacta (SNpc) and attendant striatal terminals, the presence of large protein-rich neuronal inclusions containing fibrillar α-synuclein, and an increased number of activated microglia (Tolleson and Fang, 2013). The clinical features of PD are bradykinesia, rigidity, tremor, gait dysfunction, and postural instability. Motor dysfunction is associated with the loss of 60–70% of DA neurons in the SNpc, and a decrease of up to 70–80% of the normal DA content in the striatum in clinical stage of pathology (Riederer and Wuketich, 1976). The pre-symptomatic (preclinical) stage can last for decades until about half of the DA neurons have died (Bezard et al., 2001).

PD exists in different familial and sporadic forms (Davie, 2008). Only about 10% of PD cases are accounted for by the familial form, while 90% are sporadic or idiopathic. The pathogenesis of both familial and sporadic PD is associated with failure of the ubiquitin-proteasome

system (UPS) to degrade misfolded and aggregated proteins within neurons (Ciechanover and Kwon, 2015). The age-related decline in activity of the UPS promotes the accumulation of poorly degraded proteins within cells. The long lifespan of neurons results in the continuous accumulation of these proteins, and renders them more vulnerable to the formation of pathological protein aggregates. This is one of the major reasons for the elevated frequency of sporadic PD with increasing age (Tydlacka et al., 2008). In rare hereditary PD, mutation of the UPS component Parkin could directly lead to pathological α-synuclein accumulation, accelerated neuronal loss, and instigate earlier onset of the disease (Shimura et al., 2001). In addition, rare mutations of the UCH-L1 deubiquitinating enzyme also have been shown to be associated with familial early-onset PD (Das et al., 2006). A mutant form of α-synuclein is the major pathogenic agent of PD (Singleton et al., 2003).

Most cases of PD occur sporadically. Exposure to environmental toxins is now thought to be a causative factor (Ascherio and Schwarzschild, 2016). The proteasome inhibitors lactacystin (LC) and epoxomicin are widely distributed in the environment. They are synthesized by microorganisms (*Streptomyces sp.*) that infect soil and aquatic habitats in gardens and farmlands (Kisselev and Goldberg, 2001). They have lipophilic properties and are able to penetrate the human body with food, water, and even dust. Analysis of post-mortem samples obtained from patients with sporadic PD indicate structural and functional defects in the 26/20S proteasome (Bukhatwa et al., 2010; McNaught et al., 2002). The link between proteasomal inhibition and PD pathogenesis has been further verified by the demonstration that dose-dependent treatment with the proteasomal inhibitor LC results in the formation of α-synuclein and ubiquitin-positive inclusions in rat ventral mesencephalic primary neurons, followed by neurodegeneration and microglial activation (McNaught et al., 2002, 2004; Bentea et al., 2017).

Intracellular protein homeostasis is achieved by the coordinated action of two intricate evolutionarily ancient systems, UPS and molecular chaperones, which, together, maintain protein quality control in living cells. The molecular chaperones, the majority of which are heat shock proteins (HSPs), guide proteins through different conformational changes, such as de novo folding, assembly and disassembly, transport, and targeting for degradation (Hartl et al., 2011). Malfunctions of these systems may result in a number of neurodegenerative diseases. The first evidence for the involvement of chaperones in PD was provided by studies that identified chaperones as Lewy body components (Auluck et al., 2002; Gao et al., 2015).

During the past 10 years, data have accumulated that support the neuroprotective effect of chaperones in PD models. Expression of HSP70 was shown to reduce the death of DA neurons in the α-synuclein model of PD in *Drosophila sp.* (Auluck et al., 2002). In the MPTP (1-methyl-4-phenyl-1,2,3,6-tetrahydropyridine) mouse model, elevation of HSP70 was shown to increase dopamine and tyrosine hydroxylase (TH) levels in the striatum (Dong et al., 2005), and to prevent disturbances in mouse motor behavior (Jung et al., 2008).

The sporadic form of PD usually develops in late age (De Lau and Breteler, 2006), concomitant with a loss of function in both the chaperone system and UPS (Labbadia and Morimoto, 2015). It has been demonstrated that in PD, the expression of some chaperones is reduced in the SNpc and within nigral neurons, reflecting a reduction in the control of the conformation of neuronal proteins and cellular defense mechanisms (Chu et al., 2009). This led us to hypothesize that reduced HSP70 in SNpc neurons could be a major factor that accelerates the pace of the neurodegenerative process in the nigrostriatal system in PD, and that the expression of HSP70 is required for the survival of DA neurons. The aim of this study was to develop new neuroprotective approaches to PD therapy based on inducible HSP70.

2. Material and methods

2.1. Vectors, HSP70 inducers, cells

Plasmids for HSP70 (HSPA1A) knock-down were purchased from Open Biosystems (clones TRCN0000008513 – shRNA, mature antisense: TTGATGCTCTTGTTCAGGTCG), Packaging (Δ8.91) and envelope (pVSV-G) plasmids were kindly provided by Dr. L. Glushankova (Institute of Cytology of Russian Academy of Sciences, Russia). HEK-293 T cells were transfected using PEI (polyethylenimine) with a mixture of all three plasmids. Supernatants of the cultures were harvested and concentrated using PEG/NaCl solution. Lentiviral titers were determined by estimating the number of Puromycin-resistant cell colonies.

The HSP70 inducer, U-133, was previously selected from the library of small molecule compounds of the Pacific Institute of Bioorganic Chemistry, Russian Academy of Sciences. U-133 is an acetylated tris-O-glucoside echinochrome, and is the main pigment in sea urchins. U-133 was found to induce profound synthesis and accumulation of HSP70 in human U-937 promonocytes (Lazarev et al., 2011).

To evaluate the most effective concentration of U-133, we used a reporter system based on HeLa cells bearing the luciferase gene under the HSE heat shock promoter. Cells were kindly provided by Prof. Morimoto (North Western University, USA).

2.2. Animals

Male Wistar rats, 7–8 weeks old, weighing 180–220 g, were used in these experiments. The rats were housed in individual cages under standard environmental conditions (12:12 h light:dark cycle; ambient temperature 22 ± 2 °C; food and water were available ad libitum). Motor testing was conducted between 09:00 and 15:00. The experiments were approved by the local animal care committee (Identification number F18–00380) and met the requirements of the European Communities Council Directive.

2.3. Surgery

Guide cannulas were implanted for bilateral drug infusion into the SNpc. Rats were anaesthetized with intramuscular injection of Zoletil-100 (50 mg/kg, tiletamine hydrochloride and zolazepam; Virbac, Carros, France) and placed into a stereotaxic apparatus. Stainless steel guide cannulas (internal diameter 0.3 mm) were implanted into the SNpc according to the following coordinates: 5.0 mm posterior, 2.0 mm lateral, and 7.5 mm below the bregma (Paxinos and Watson, 1986). The guide cannulas were secured with dental cement. After surgery, animals were returned to their home cages and allowed to recover for 7 days.

2.4. Proteasome inhibitor treatment

The irreversible proteasome inhibitor lactacystin (LC; Enzo Life Sciences, USA) was diluted in apyrogenic phosphate-buffered saline (PBS) to final concentrations of 0.4 μg/μl or 4 μg/μl. Immediately before use, PBS was filtered through a sterilized syringe filter (30 mm, PVDF, 0.22 μm; JET BIOFIL®, Korea). LC was injected immediately after dilution. The rats were lightly anaesthetized with Zoletil (30 mg/kg) before the injection. Two successive bilateral LC microinjections into the SNpc (0.4 or 4 μg) were performed with a 1-week interval, using a 1 μl Hamilton syringe (Hamilton, Reno, NV, USA) connected to the guide cannula. LC was injected at a volume of 1 μl and a flow rate of 0.1 μl/min. Control rats were treated similarly but received an equivalent volume of vehicle instead of LC.

2.5. HSP70 gene down-regulation

To understand how reduction of HSP70 levels in DA neurons

impacts degeneration, we used 5 groups of rats; animals were injected through the guide cannulas as described above with (1) 1 µl vehicle ($n = 6$), (2) a lentiviral construct carrying the green fluorescent protein (GFP) gene ($n = 6$), (3) lentiviral construct carrying the shHSP70 RNA only ($n = 6$), (4) LC alone ($n = 6$), and (5) both shHSP70 RNA and LC ($n = 6$). LC was first injected 2 weeks after shHSP70, and again 7 days later (see Fig. 2A for explanation).

2.6. U-133 treatment

HSP70 inducer, U-133, was diluted in 20 µl DMSO and 0.2 ml 0.9% NaCl prior to each administration. The rats ($n = 7$) were treated with U-133 (5 mg/kg, i.p.) 4 h and 24 h after each LC microinjection, and 7 days after the last LC microinjection. In control experiments, the vehicle of U-133 DMSO was used instead of U-133 ($n = 7$). U-133 was also introduced to untreated LC animals ($n = 7$).

2.7. Behavioral assessment of motor dysfunction of rats

Rats were videotaped and then examined 2 weeks after the final microinjections (LC or vehicle) into the SNpc, to determine the presence, severity, and progression of motor dysfunction.

2.8. Sunflower seed test

The sunflower seed test is an easy way to assess and quantify motor dysfunction associated with fine movements of the fore-limbs, mouth, and tongue (Gomez et al., 2006; Kane et al., 2011). Two days before the test, rats were trained to eat sunflower seeds in their individual home cages. On the day of the test, each rat received 35–40 sunflower seeds after 24 h of food deprivation. The experimenter began timing when the animal touched the first seed. The number of sunflower seeds eaten in 5 min was counted.

2.9. Suok test

The Suok test simultaneously assesses rodent motor dysfunction and coordination disturbances (Kalueff et al., 2008). At the beginning of each trial, the rat was placed on the end of a bar (150 cm length; 3.5 cm width) elevated to a height of 45–50 cm above a cushioned test surface. The home cage of the rat was placed on the opposite end of the bar. Motor coordination and changes in the gait of the animal were assessed while the rat was moving along the bar. The number of hind-limb missteps during 3 trials were counted. The severity of motor disorder was evaluated according to a modified rating scale (Mittoux et al., 2002): coordination: 0 points, normal coordination; 0.5 points, hind-limb misstep; 1 point, slipping from the bar with hanging; 2 points, falling from the bar; 3 points, inability to move along the bar; gait: 0 points, normal, active gait; 1 point, wobbling gait; 2 points, uncoordinated gait with widely spread limbs; 3 points, hind-limbs unable to sustain walk and body weight but fore-limbs able to keep upright position balance.

2.10. Inverted horizontal grid test

An inverted horizontal grid test was used for the assessment of sensorimotor deficits of limbs (Smith et al., 2001; Tillerson et al., 2002). The rat was placed on a horizontal grid (22×13 cm, cells 0.5 cm^2) positioned at a height of 40 cm above a cushioned test surface. The experimenter turned the grid over and started the stopwatch. The number of seconds of grid hanging using all four limbs was recorded.

2.11. Brain sample preparation

At the end of the experiments, after the motor tests (21 days after the first microinjection of LC or vehicle into the SNpc), the rats were anaesthetized with Zoletil-100 (50 mg/kg, i.m.) and decapitated. One half of each brain was fixed in 4% paraformaldehyde for immunohistochemical assays. The second half was used to dissect the SNpc, motor cortex, and dorsal striatum, which were kept at −70 °C for further biochemical analysis. Four h after bilateral microinjections of LV, which expresses GFP into the SNpc, the rats were anaesthetized and rapidly transcardially perfused with 4% paraformaldehyde in PBS. The brain was extracted and examined by confocal microscopy for the presence of LV, which expresses GFP. Brains from all animals used for immunohistochemical assays were fixed in 4% paraformaldehyde and cryoprotected in 20% sucrose before storage in isopentane at −70 °C. Coronal sections (10 µm) were prepared for morphological and immunohistochemical assay with a Leica CM1510S-1 cryostat (Leica Microsystems, Nussioch, Germany). The frontal slices were collected at the level of the SNpc (from bregma −4.80 to −5.80) according to the atlas of Paxinos and Watson (Paxinos and Watson, 1986). Six alternate series of sections were mounted on SuperFrost_Plus slides (Menzel GmbH, Brunswick, Germany).

2.12. Immunohistochemistry

For bright-field microscopic analysis, sections were preincubated first with 3% H$_2$O$_2$–10% methanol for 20 min, and then with 3% normal goat serum (NGS) and 0.3% Tween-20 for 1 h at room temperature. Sections were incubated for 48 h at room temperature with primary antibodies against TH (1:900; rabbit, Abcam, UK), VMAT2 (1:100; Sigma-Aldrich, USA), inducible HSP70 (Clone 3C5, specific to human, mouse, and rat HSP70, Lasunskaia et al., 2010), and Iba-1 (1:250; Abcam, UK). Incubation with biotinylated secondary antibodies was followed by incubation with streptavidin–peroxidase (1:250; Vector Labs., USA). Reactions were visualized using 3,3-diaminobenzidine (Sigma-Aldrich, USA) as a chromogen. Additionally, reactions lacking primary antibodies were performed to ensure the specificity of the observed staining. Immunostained sections of SNpc were examined in a conventional microscope (Karl Zeiss, Germany) and recorded with a digital camera (Imager 4.1) controlled by AxioVision (4.8) software.

For confocal microscopy, sections were preincubated in blocking solution (2% bovine serum albumin and 2% NGS diluted in PBS with 0.1% Tween-20 (PBST) for 1 h at room temperature, and then incubated with a primary rabbit anti-TH antibody (1:900; rabbit, Abcam, UK), and mouse anti-HSP70 (Clone 3C5), for 24 h at room temperature. After rinsing in PBS, the sections were incubated for 2 h at room temperature with secondary antibodies labeled with DyLight 488, DyLight 549 antimouse, or anti-rabbit IgG (1:350 for all; Thermo Scientific, USA). Double immunofluorescence staining for TH (1:300; mouse, Sigma-Aldrich, USA) with α-synuclein (1:200; rabbit, Novus Biologicals, USA) was also used. Reactions were visualized with anti-mouse DyLight 549 for TH and anti-rabbit DyLight 488 for α-synuclein; they were subsequently incubated with 4′,6-diamidino-2-phenylindole (DAPI) for 2 min (1:1000; Sigma-Aldrich, USA). Fluorescent images were captured by a Leica TCS SP2 confocal system (Leica, Germany). Unlabeled sections were used to determine autofluorescence. To avoid possible cross interference among the various fluorochromes, images for Alexa-555, DyLight 488, DyLight 549, and DAPI were acquired using the sequential image recording method.

2.13. Immunoblotting

Tissues were homogenized in lysis buffer containing a protease inhibitor cocktail (Sigma Aldrich, St. Louis, MO, USA). Electrophoresis was performed in 11% polyacrylamide gel according to a standard protocol. Protein bands were transferred onto PVDF membranes of pore size 0.45 µm (Millipore, Germany), with a TransBlot apparatus (BioRad, USA). The membranes were stained with monoclonal anti-HSP70 (mouse, Clone 3C5), and monoclonal anti-Hdj1 antibody (mouse, Clone

J32) and with the antibodies against GAPDH or beta-tubulin (Abcam, UK) as loading controls, and subsequently with secondary antibodies conjugated with peroxidase (Abcam, UK). Visualization of the bands was performed using a chemiluminescence protocol.

2.14. Filter trap assay

SNpc lysates were incubated in the presence of 2% sodium dodecyl sulfate (SDS) at 98 °C for 2 min, and then equal amount of protein lysate (300 μg) from each sample was filtered through a 0.22 μm cellulose acetate membrane using a 96-well TransBlot manifold (BioRad, USA). The membrane was pre-equilibrated with washing buffer containing 10 mM Tris HCl pH 8.0, 150 mM NaCl, and 0.1% SDS, and then incubated in PBS containing 5% fat-free milk and 0.1% Tween-20, then probed with the antibody against α-synuclein (rabbit, Novus Biologicals, USA).

2.15. Image analysis

The number of TH-positive cell bodies that extended rostrocaudally with visible nuclei in the SNpc were counted and expressed as the average number of positive stained neurons per SNpc section. Quantification was carried out using 8–10 sections at the same level of the studied zones, from each animal, separated by approximately 70 μm. Anatomical sites were identified using the atlas of Paxinos and Watson (Paxinos and Watson, 1986). The analysis was performed using the PhotoM freeware (http://www.t_lambda.chat.ru/).

In addition to quantitative analysis, semi-quantitative analysis was used for the estimation of optical density of the TH, VMAT2, or HSP70 immunoreactivity in individual nigral cell bodies, using the PhotoM freeware. The sections were processed under standardized conditions in each experiment, i.e. control and experimental groups in each experiment were collected, fixed, and then processed for immunohistochemistry, simultaneously. Maintaining this order for the sample preparation allowed semi-quantitative analysis of protein levels in the histological slices by measurement of optical density (Taylor and Levenson, 2006). Five sections at the same level of the studied zones were analyzed from each animal. On each image, the immunopositivity of TH, VMAT2, or HSP70 associated with neurons was separated manually from the background. The optical density, reflecting the content of immunopositive substance, was calculated as the "grey level" of immunoreactive SNpc neurons minus background "grey level". Optical density of the background was estimated in the same slice of brain tissue in a non-immunoreactive field. Results were presented in relative units of optical density per μm^2.

2.16. Statistics

All data were analyzed using Statistica 7.0 software (Stat Soft Inc., USA) and expressed as the mean ± standard error of the mean (SEM). Behavioral data were compared using the Mann–Whitney non-parametric test. For immunohistochemistry and for Western blot analysis, one-way ANOVA and Fischer's LSD post hoc test was performed. A statistical difference was determined by a value of $p < 0.05$.

3. Results

3.1. Knock-down of HSP70 (HSPA1A) in dopaminergic neurons aggravates their degeneration and reduces compensatory mechanisms in the rat PD model

Lactacystin (LC) is a microbial metabolite that irreversibly inhibits the activity of proteasomes and causes the development of PD-like pathology in animal models (Bentea et al., 2017). In this study, the injection of 0.4 μg or 4.0 μg of LC into the SNpc led to the dose-dependent death of 20–30% or 60–70% of DA neurons in the SNpc,
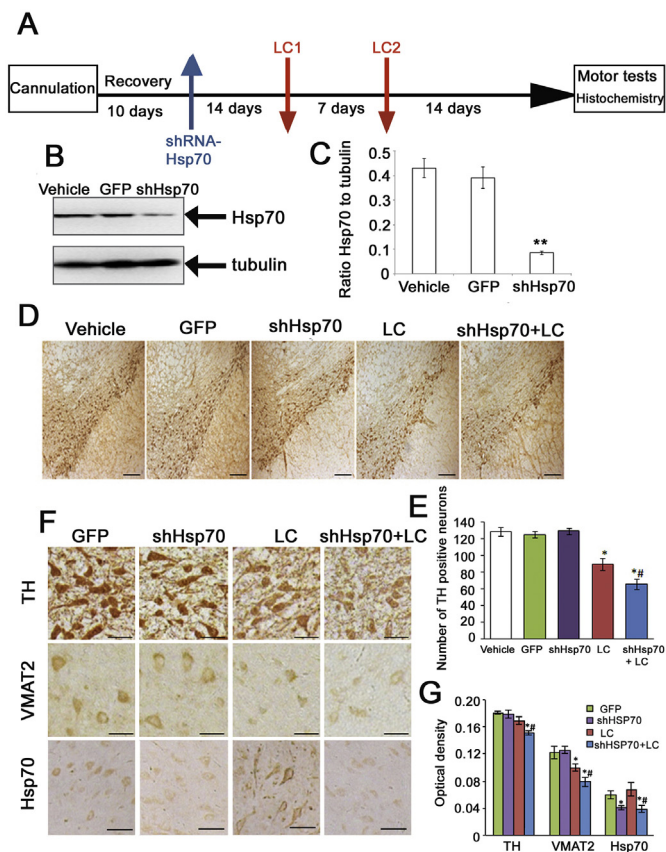

Fig. 1. Target delivery of a lentivirus bearing HSP70 shRNA knocks down HSP70 expression and leads to augmented neurodegeneration in the Substantia nigra pars compacta (SNpc) of rats in the lactacystin (LC) model of preclinical stage of PD. (A) Schematics of the experiment. (B) Western blot of SNpc from rats injected with vehicle ($n = 3$), lentiviruses expressing GFP ($n = 3$), or shHSP70 RNA ($n = 3$). (C) The intensity of bands from B were estimated using TotalLab Quant software. A representative Western blot is shown. (D and F) Brain slides from experimental groups were stained with antibodies against TH, VMAT2, or HSP70. Six animals from each group were used for analysis. Representative images are shown. Quantitative analysis was performed by PhotoM freeware. (E) The number of TH-containing neurons. (G) Optical density of TH, VMAT2, or HSP70 immunoreactivity in individual nigral cells. Optical density was estimated by PhotoM freeware. Scale bars - 50 μm. *$p < 0.05$, **$p < 0.01$ vs. the GFP-expressing group; #$p < 0.01$ vs. the LC group model of the PD-like clinical stage in rats.

respectively, thus suggesting the development of neurodegeneration imitating preclinical or clinical stages of PD pathology.

Since HSP70 constitutes the powerful protective system acting in DA neurons, we hypothesized that a reduction of the chaperone could provoke progression of neurodegeneration in the LC model of PD. To test this, we knocked down HSP70 expression in SNpc neurons using a recombinant lentivirus (LV) that expresses shRNA-HSP70. LV expressing shRNA-HSP70 was administrated into the SNpc; 14 days later, 0.4 μg of LC was injected repeatedly every 7 days (Fig. 1A). Twenty-one days after the first injection of LC, rats were sacrificed and brain slices were obtained for immunohistochemical analysis with antibodies against tyrosine hydroxylase (TH), vesicular monoamine transporter 2 (VMAT2), and HSP70. To verify that the shRNA-HSP70 caused a decrease in HSP70 in the SNpc, we used immunoblotting with antibody against inducible HSP70 (Fig. 1B).

Quantitative analysis of immunoblots of nigral tissues showed that HSP70 was reduced by 66.7% ($p < 0.01$), compared to GFP and vehicle controls (Fig. 1C). Targeted delivery has been confirmed in a pilot experiment (Suppl. Fig. 1S).

The number of TH-positive neurons in the SNpc in rats injected with

LC was reduced by 28–30% ($p < 0.05$) when compared to vehicle and GFP controls (Fig. 1D and E). Such a level of neurodegeneration mimics the preclinical stage of PD. HSP70 knock-down caused a 1.7-fold increase in the death of SNpc DA neurons ($p < 0.05$) compared to LC alone (Fig. 1D and E); such a level of neuronal death has been shown to be associated with the clinical stage of PD (Bezard et al., 2001).

To evaluate the functional state of surviving SNpc neurons, we measured the TH optical density, which reflects the activity of the DA system, the optical density of VMAT2, which loads dopamine into synaptic vesicles, and the HSP70 optical density, which reflects the neuroprotective potential. The reduction in TH optical density in SNpc neurons after two LC injections was not statistically significant, whereas knock-down of HSP70 in rats injected with LC led to a decrease in TH by $16.5 \pm 1.3\%$ ($p < 0.05$). The VMAT2 level in LC injected rats was decreased by $18.0 \pm 2.2\%$ compared with control GFP-expressing animals, and reduced even further, by $35.2 \pm 0.9\%$ ($p < 0.01$), after knock-down of HSP70 (Fig. 1F and G). Interestingly, infection with shHSP70 alone did not cause cell death in the SNpc, nor did it influence the level of TH and VMAT2 in DA neurons. As expected, the HSP70 content in surviving neurons was reduced in knocked-down animals. (Fig. 1F and G).

An increase in SNpc neurodegeneration and an attenuation of compensatory mechanisms for neuronal survival were correlated with disturbance of motor behavior in rats with down-regulated HSP70. Using the sunflower seed test, which reflects disturbance of fine motor functions of fore-limbs, mouth, and tongue, we found that control animals were able to eat 18.5 ± 1.0 seeds during 5 min, and the capacity of the rats in the preclinical stage of PD (treated with LC alone) was unaffected, as they consumed 15.0 ± 1.5 seeds during the same time period. The rats with down-regulated HSP70 which were treated with LC showed a 2-fold decrease in their capacity to eat seeds (Fig. 2A).

Using the Suok test, which reflects motor dysfunction and

Fig. 2. Knocking down HSP70 in rat Substantia nigra pars compacta (SNpc) leads to motor disturbances in the lactacystin (LC) model of Parkinson's disease. (A) Sunflower seed test; (B and C) Data from the Suok test; (D) Inverted horizontal grid test. * $p < 0.01$ vs. GFP-expressing group; # $p < 0.01$ vs. the LC group.

coordination disturbance, we found that only animals with down-regulated HSP70 demonstrated significant difficulties: the number of hind-limb missteps was 4-fold higher compared with control GFP-expressing animals (Fig. 2B), and the severity of motor disturbance was 2.3 points higher (Fig. 2C). These parameters were not affected significantly in animals treated with LC only (Fig. 2B and C). To evaluate the sensorimotor deficits of limbs, we used the inverted horizontal grid test, which measures hanging time, and found that the hanging time of animals with down-regulated HSP70 was 1.6 ± 0.2 s, whereas the hanging time of control animals and rats treated with LC was 14.2 ± 2.0 s and 12.2 ± 2.0 s, respectively (Fig. 2D). Importantly, shRNA-mediated reduction of HSP70 content in the SNpc without treatment with LC did not affect motor function (Fig. 2).

In conclusion, HSP70 knock-down in the SNpc significantly accelerated DA neuron degeneration, which may reflect transition of the pathology from the preclinical to the clinical stage of PD.

3.2. Increase in HSP70 and Hdj1 levels in the PD-imitating neurons ameliorates their physiological function

The data presented in the previous section suggest that inducible HSP70 is a key element in neurodegeneration in the LC model of PD, and induction of its expression could counteract neurodegeneration and provide therapeutic efficacy.

Recently, we analyzed a library of small molecules from Pacific Institute of Bioorganic Chemistry of the Far East Branch of the Russian Academy of Sciences consisting of groups of compounds of natural origin, and discovered that the U-133 echinochrome derivative was able to induce HSP70 and Hdj1 synthesis in mammalian cells (Lazarev et al., 2011). Recently, we have shown that U-133 is able to reduce tumor growth in mice (Yurchenko et al., 2015).

Using HeLa cells bearing a reporter plasmid that expresses luciferase under the control of the HSE-promoter, we found that U-133 activated HSE in a dose-dependent manner, and caused the activation of the HS promoter at a concentration of 10 μM better than heat shock does (Fig. 3A). U-133 did not cause any notable changes in food behavior and body weight of experimental animals and displayed little cellular toxicity: IC_{50} in 3 T3 mouse fibroblasts was 74,5 μM (Suppl. Fig. 2S). Guided by this data, we chose the concentrations of 0.5 and 5 mg/kg, which approximately corresponds to 1 and 10 μM, respectively. We then estimated the ability of U-133 at these concentrations to increase HSP70 and Hdj1 in brain structures. Rats were injected with U-133 intraperitoneally, and were sacrificed 24 h later. The level of HSP70 and its co-chaperone Hdj1 in the striatum and in SNpc was measured using immunoblotting with anti-HSP70 and anti-Hdj1 antibodies. Both HSP70 and Hdj1 in the striatum and SNpc of U-133-treated animals were elevated in a dose-dependent manner. At a maximum U-133 dose of 5 mg/kg, the HSP70 (and Hdj1) in these structures increased 3.1- and 4-fold (3.9- and 2.4-fold), respectively. This dose was chosen for further experiments.

To determine whether administration of the U-133 HSP70 inducer was therapeutically efficacious, we used it in the LC model of PD imitating clinical stage. Rats were injected with U-133 4 and 24 h after each LC microinjection. A dose of 4 μg of LC was injected into the SNpc twice, with a 7-day interval (see Fig. 4A for explanation). Additional injection of U-133 was performed 7 days after the last LC microinjection. Twenty-one days after the first LC microinjection, behavior tests were performed and the animals were sacrificed for further immunohistochemical and biochemical analyses.

Double LC microinjections led to the death of $60.7 \pm 1.4\%$ of SNpc DA neurons in the rats (Fig. 4B and C), mimicking the clinical stage of PD. The treatment with U-133 reduced the number of dying DA neurons 2.3-fold (Fig. 4B and C). U133 did not change the amount of TH-positive neurons in the SNpc in LC untreated rats.

Microinjection of LC reduced the optical density of TH in the remaining neurons by $15.8 \pm 1.0\%$, and VMAT2 by $20.0 \pm 0.8\%$, in
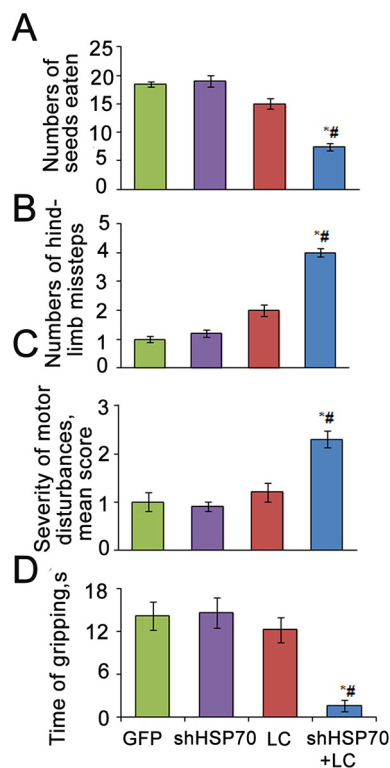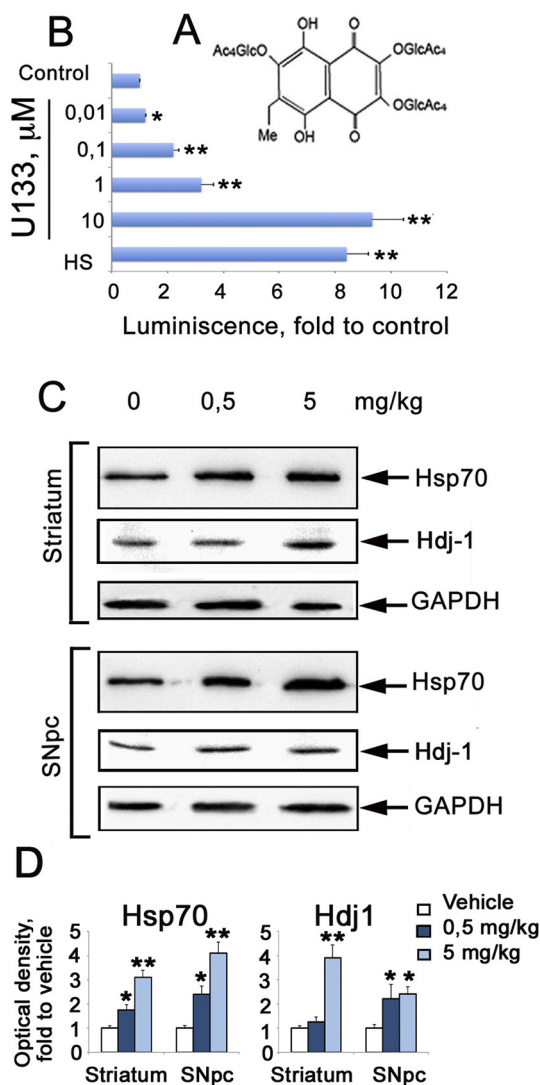
Fig. 3. Echinochrome derivative (U-133) causes dose-dependent elevation of HSP70 in the striatum and Substantia nigra pars compacta. (A) Activation of the HSE promoter in the luciferase reporter system in HeLa cells. U-133 was used in the titers indicated. HS – heat shock, 43 °C, 30 min. (B) Western blot analysis of brain structures from animals treated with U-133 at two doses ($n = 3$ in each case) with the antibodies against Hsp70 and Hdj1. (C) The intensity of bands from B were estimated with the TotalLab Quant software. Statistical significance is indicated as * $p < 0.05$, ** $p < 0.01$.

comparison to vehicle control (Fig. 4D and E). The treatment with U-133 prevented the decrease in TH and VMAT2. HSP70 was decreased in DA neurons in LC treated rats by $21.6 \pm 0.8\%$ compared to the chaperone level in healthy animals. The treatment with U-133 prevented the reduction of the chaperone level in neurons of the SNpc (Fig. 4D and E). The treatment with U-133 led to an increase of TH content by $9 \pm 0.7\%$, and HSP70 by $55 \pm 1.7\%$, in DA neurons in the SNpc of healthy rats (Fig. 4D and E).

We analyzed the motor behavior of experimental animals and found that rats administered LC were significantly impacted in terms of fine motor functions of the fore-limbs, mouth and tongue, as demonstrated by a 1.6-fold diminished ability to eat seeds during a defined time interval, compared to control rats (Fig. 4F). Further, the number of hind-limb missteps was 7-fold higher in these rats, the severity of their motor disturbance reached 6 points, and the time range of their hanging on grid was reduced 1.9-fold, compared to vehicle-treated rats. Treatment with U-133 prevented the motor malfunction induced by LC (Fig. 4G–I).

Thus, our data demonstrate that increased HSP70 content in the

SNpc with U-133 treatment reduced the development of the neurodegenerative process, prevented TH and VMAT2 decreases in DA neurons, and stopped the signs of motor deficiency, in the LC model of PD.

3.3. Insights into the mechanism of HSP70-mediated neuroprotection

One of the hallmarks of PD pathology is α-synuclein amyloid fibril formation in Lewy bodies within nigral neurons (Braak et al., 2003). It is well known that neuronal death is caused by α-synuclein oligomers and toxic protofibrils (Roberts and Brown, 2015). Heat shock proteins are associated with α-synuclein and other amyloidogenic proteins in oligomeric states, and suppress fibril formation (Balchin et al., 2016). Therefore, we tested the most plausible effect of α-synuclein aggregation in our model of PD, as well as the participation of inducible HSP70 and its co-chaperone Hdj1 in amyloid disassembly, and its impact on PD pathophysiology. To reveal the aggregation, we stained DA neurons of the SNpc with an anti-α-synuclein antibody in animals treated with LC, and found that the inhibition of proteasomes, indeed, caused aggregate formation; the aggregation was a specific feature of DA neurons and was not observed in brains of animals treated with vehicle alone (Fig. 5A). Formation of α-synuclein aggregates was also demonstrated with the aid of the Filter Trap Assay (Fig. 5B). Treatment with U-133 reduced α-synuclein aggregates, as visualized by confocal microscopy (Fig. 5A), by virtue of its ability to induce HSP70. These findings were further confirmed with the Filter Trap Assay; U-133-mediated HSP70 accumulation led to a > 2-fold reduction in stained anti-α-synuclein antibody, SDS insoluble material retained on the membrane (Fig. 5B and C). Notably, a long time course of treatment was necessary to achieve therapeutic effects, as two consistent treatments of U-133, 4 and 24 h after the first microinjection of LC, did not have a significant influence on aggregation of α-synuclein (Fig. 5B and C, upper panels).

To understand why a prolong U-133 administration is needed to achieve disaggregation of α-synuclein in SNpc neurons, we examined how long the elevated levels of Hsp70 and Hdj1 remained in SNpc after a single dose of U-133. We injected C57Black mice with 5 mg/kg of U-133 and monitored Hsp70 and Hdj1 in SNpc 1, 3, 7 and 10 days post-injection by Western blotting (Fig. 5D,E). Contrary to highly proliferating U-937 cells (Lazarev et al., 2011), the SNpc levels of both proteins remained high during 7 days post-treatment and then slowly decreased (Fig. 5D,E). We conclude that to reach a potent therapeutic effect it is necessary to sustain a high level of chaperones in SNpc for an extended amount of time.

HSP70 likely interacts directly with the aggregates (Kim et al., 2002) to interfere with α-synuclein fibrils in neurons affected by the proteasome inhibitor. To test this, we stained the SNpc with anti-HSP70 and anti-α-synuclein antibodies. We observed α-synuclein aggregates in animals treated with LC; in contrast, there was an even distribution of the protein in untreated cells (Suppl. Fig. 3S). Induction of HSP70 synthesis caused a dramatic reduction in the number of α-synuclein aggregates, and the HSP70 colocalized with α-synuclein, particularly in neurons of LC treated animals, suggesting its possible involvement in the aggregate organization or disassembly (Suppl. Fig. 3S).

Another feature of PD is inflammation and microglial activation, which contributes to the development of neurodegeneration in PD (Béraud et al., 2013). To test microglia activation in the LC model, we used antibodies against the microglial marker Iba1 to calculate the number of Iba1-immunopositive cells. We observed that microinjection of LC caused a 186% increase in Iba1-positive cells in the SNpc, compared to the animals treated with vehicle (Fig. 5E). Conversely, U-133 treatment decreased microgliosis, as shown by a 1.5-fold decrease in Iba1-positive cells (Fig. 5F).

4. Discussion

In this study we demonstrated that LC microinjection into the SNpc in various doses was able to imitate the molecular and behavioral
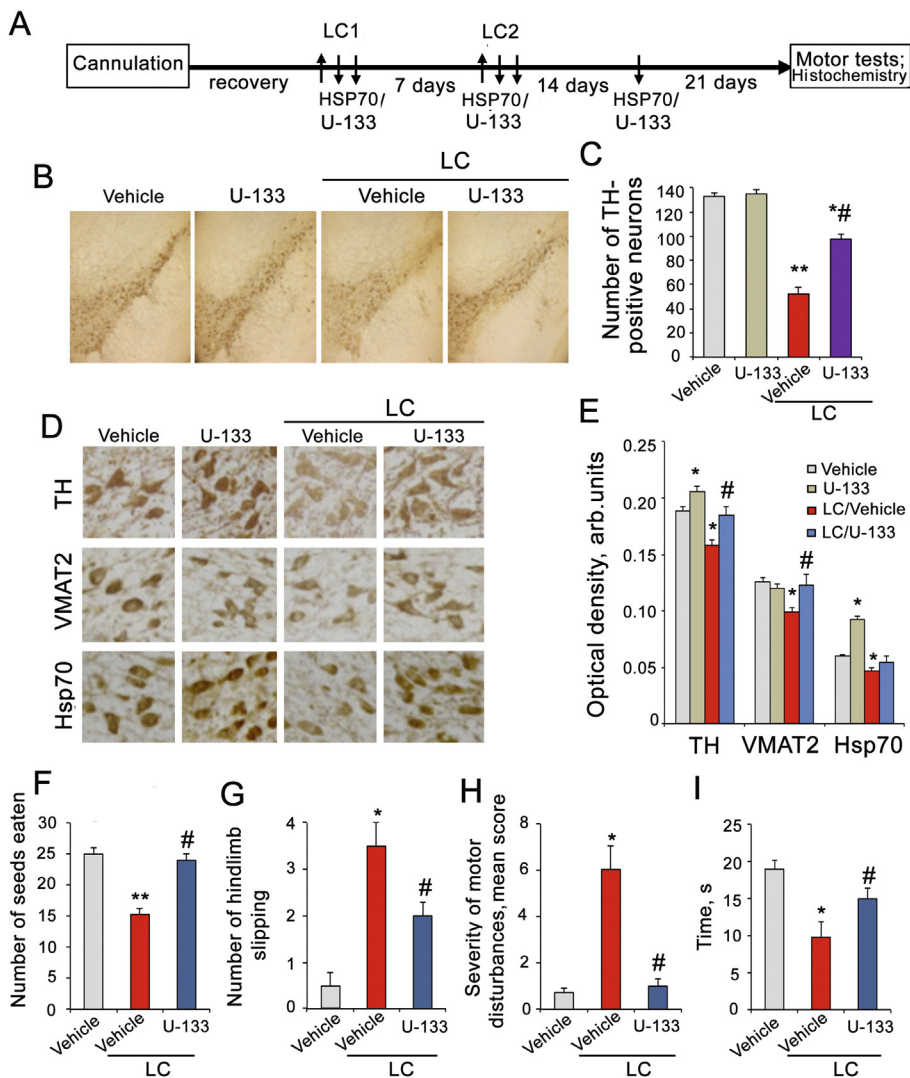
Fig. 4. Treatment of PD-like animals in clinical stage with U-133 attenuates neurodegeneration in the Substantia nigra pars compacta, stimulates the compensatory mechanisms directed to maintain the dopamine level in dopaminergic neurons, and prevents motor dysfunction. (A) Schematics of the experiment. (B) Brain slides from experimental groups were stained with an antibody against TH. Seven animals from each group were used for analysis. Representative images are shown. (C) Quantitative analysis was performed by PhotoM freeware. (D) Brain slices treated as in A were stained with TH, VMAT2, or HSP70 antibodies. (E) Optical density of TH, VMAT2, or HSP70 immunoreactivity in individual nigral cells. Scale bars - 50 μm. * $p < 0.05$, ** $p < 0.01$ vs. the vehicle injected group ($n = 7$); # $p < 0.01$ vs. the LC group ($n = 7$). Motor disturbances in the LC model of PD were evaluated with aid of the Sunflower seed test (F), Suok test (G), and the inverted horizontal grid test (H and I) * $p < .01$ vs. the vehicle injected group; # $p < 0.01$ vs. the LC group.

abnormalities of PD in a rat model. The LC model recapitulated the major pathomorphological hallmarks of PD, such as the loss of SNpc DA neurons, α-synuclein aggregation, increased amount of activated microglia, and motor dysfunctions. At the molecular level, TH and VMAT2 were diminished (Fig. 1). The important advantage of LC model is that two different concentration of the proteasome inhibitor give rise to preclinical and clinical phase simulations of PD. To evaluate the therapeutic potential of HSP70, we modulated its abundance in DA neurons by down- and up-regulation.

To understand whether HSP70 may play a role in the development of PD, we down-regulated its expression in the SNpc with specific shRNA. Using a rat model resembling the preclinical stage of PD, we found that HSP70 knock-down increased the vulnerability of nigral DA neurons, and accelerated neurodegeneration (Fig. 1); neuronal death was dramatically elevated, and compensatory mechanisms directed to maintain dopamine levels in neurons were diminished, as indicated by the low expression of TH and VMAT2 (Fig. 1). Animals with down-regulated HSP70 in the SNpc displayed impaired motor coordination and balance (Fig. 2). Loss of HSP70 function due to a mutation in the ATP-binding domain has been reported to accelerate the pathological phenotype in flies under α-synuclein overexpression (Auluck et al., 2002). In another study, siRNA-mediated down-regulation of GRP78, a close relative of HSP70, aggravated α-synuclein neurotoxicity in rat nigral DA neurons (Salganik et al., 2015). In summary, the loss or dysfunction of HSP70 family members appears to play an essential role

in PD pathology by augmenting the symptoms.

The neuroprotective effects of HSP70 demonstrated in our study are consistent with results from earlier studies (Auluck et al., 2002; Jung et al., 2008; Ahn and Jeon, 2006). Our results confirm the hypothesis that HSP70 elevation is a promising therapeutic treatment for PD. Most previous studies were performed using viral vectors to deliver HSP70 to affected neurons. However, the use of viral vectors for HSP70 gene transfection to damaged cells is not currently in practice due to the possible side effects and associated high risk of unpredictable immune reactions (Mingozzi and High, 2011). In the past 20 years, researchers have searched for a drug capable of increasing HSP70 in brain neurons (Ebrahimi-Fakhari et al., 2011). Substances extracted from a Chinese herb and endemic Far East organisms are currently under consideration.

Several compounds, including celastrol, geldanamycin, novel synthetic squamosamide derivative FLZ and arimoclomol, have demonstrated promising therapeutic effects, in vivo and in vitro, in models of PD and other conformational pathologies (Ebrahimi-Fakhari et al., 2011; Westerheide et al., 2004; Lazarev et al., 2017; Bao et al., 2017). Despite their benefits, some of these drugs exhibit serious side effects. For example, celastrol exhibits cellular toxicity; this substance had no neuroprotective effect in both animal and cell models, while being toxic in micromolar concentrations (Konieczny et al., 2014). Geldanamycin was also shown to be hepatotoxic, and demonstrated extremely low capacity to pass the blood-brain barrier (Kalmar et al., 2014). Taken
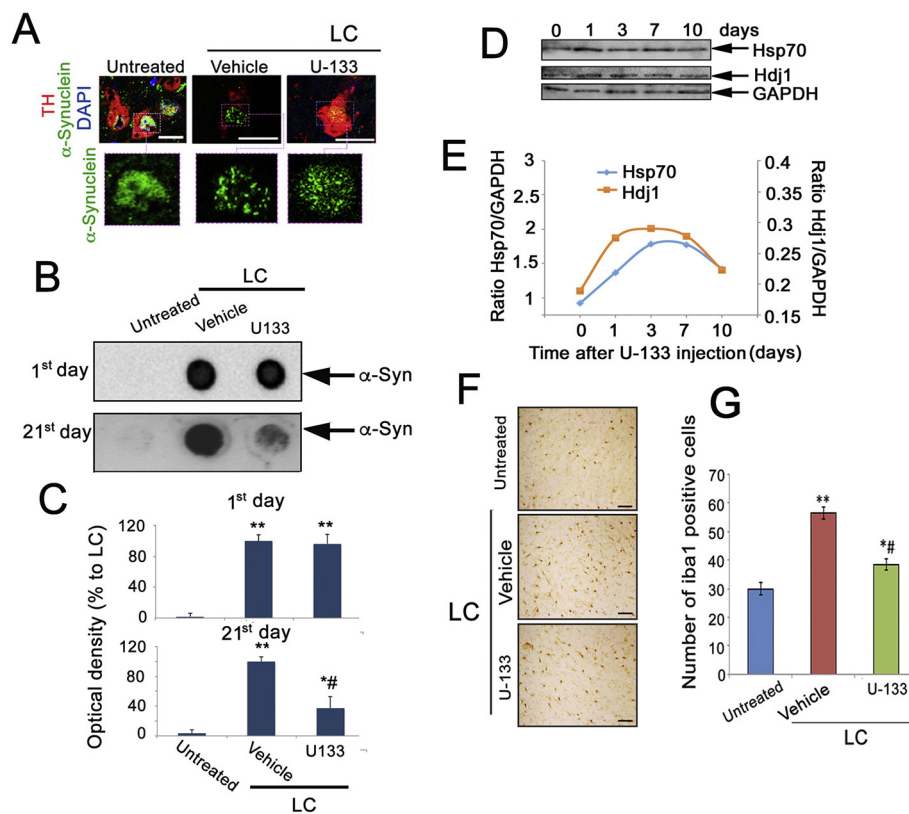
Fig. 5. Elevation of HSP70 in the Substantia nigra pars compacta (SNpc) suppresses α-synuclein pathology and diminishes neuroinflammation in the SNpc. (A) Brain slices of animals from each experimental group ($n = 3$) were stained with antibody against TH (red) and α-synuclein (green). Inserts depict α-synuclein aggregates in Lewy bodies. (B) α-synuclein aggregation detected by the Filter Trap Assay. (C) Intensities of membrane-retained fractions, as estimated by TotalLab Quant software. Representative data from three experiments is shown. $* p < 0.05$, $** p < 0.01$. (D) Western blot of SNpc in C57Black mice treated with 5 mg/ml U-133 1, 3, 7 and 10 days after single injection (E) The intensity of bands from D was measured using the TotalLab Quant software. Data is the mean from three independent experiments. (F) Slices of SNpc were stained with Iba-1 antibodies. Data from optical microscopy is presented. (G) The number of Iba-1 positive cells was estimated by PhotoM freeware. Scale bars – 50 μm. $* p < 0.01$ vs. the untreated group; $\# p < 0.01$ vs. the LC group. (For interpretation of the references to colour in this figure legend, the reader is referred to the web version of this article.)

together, these untoward side effects compelled us to pursue a search for novel and safe inducers of HSP70. One such possible candidates is the echinochrome derivative U-133, which was earlier shown to induce both HSP70, and its co-chaperone HSP40 (Hdl1), synthesis in micromolar concentrations, and to elevate their substrate-binding activities (Lazarev et al., 2011). This elevation was found to provide a protective effect on human cells subjected to oxidative stress (Lazarev et al., 2016). Importantly, the compound demonstrated its safety in experiments with cell cultures (Suppl Fig.2S), and in studies with animals (Yurchenko et al., 2015).

Using HSE-luciferase reporter assays, we found that the potential of U-133 for HSF1 activation was comparable to that of mild heat shock (Fig. 3A). Intraperitoneal injection of U-133 increased HSP70 in a dose-dependent manner in the SNpc and the striatum (Fig. 3B).

To demonstrate that the HSP70 inducer, U-133, could be therapeutically effective, we used a rat model that mimics the clinical stage of PD, and showed that U-133 decreased the loss of DA neurons by 2-fold, in comparison to untreated LC rats, protected the functional activity of SNpc neurons, and eliminated the motor dysfunction features characteristic of PD (Fig. 4).

Extracellular recombinant HSP70 has been widely used to increase HSP70 in damaged neurons since it was discovered that the chaperone is released from neurons (Tytell et al., 1986) and rat fibroblasts (Hightower and Guidon Jr, 1989); both studies prompted the use of exogenous Hsp70 in a variety of preclinical modalities. In our recent study, recombinant HSP70 administered intranasally was shown to penetrate the hippocampal neurons and prevent the development of pathological features in the genetic mouse model of Alzheimer's disease (Bobkova et al., 2014). Previously, we demonstrated that HSP70 extracted from bovine muscle penetrated into the neurons of different brain areas, including the hippocampus, piriform cortex, and the hypothalamus, and resulted in reduced severity of NMDA- and pentylenetetrazole-induced seizures (Ekimova et al., 2010). In the current study, we showed that SNpc DA neurons also incorporate extracellular HSP70 (Suppl Fig. 4S) and, similarly to U133, significantly diminished

the amount of dead DA neurons (Suppl. Fig. 5S A,C), improved the function of surviving neurons (Suppl. Fig. 5S B,D), and prevented the development of motor dysfunction (Suppl. Fig. 5S E).

HSF1 governs the expression of > 1000 genes including many of the chaperone family (Mendillo et al., 2012). The neuroprotective effect of exogenous Hsp70 was similar to that of U-133 (Suppl. Fig. 5S), suggesting that the contribution of Hsp70 is more important for neuroprotection then that of other chaperones (Bobkova et al., 2014). Downregulation of Hsp70 in C6 glioma cells via specific anti-Hsp70 (HSPA1A) shRNA abolished the Hsp70 induction during heat shock or U-133 treatment without diminishing Hdj1 (Suppl. Fig. 6S A) and eliminated the protective effect of U-133 against LC (Suppl. Fig. 6S B). Taken together these results argue that Hsp70 is the primary neuroprotective effector of U-133.

Taken together, our findings support the conclusion that U-133 used in this study as a positive regulator of HSF1 as well as exogenous Hsp70 inhibits neuronal degeneration associated with the LC model of PD. Temporary delay of the symptoms associated with the clinical stage of PD is now acknowledged as a long-term goal of contemporary pharmacological treatment (Rodríguez-Nogales et al., 2016). The survival of SNpc neurons may occur due to the activation of HSF1 and elevation of HSP70 chaperone level. Similar therapeutic effect was shown in the 6-OHDA PD model, as demonstrated by decreased loss of DA neurons, maintenance of functional DA neuron activity, and by gait improvement (Suppl. Fig. 7S).

Importantly, LC microinjection into the SNpc led to the formation of α-synuclein aggregates, which were localized mainly in the nucleus (Fig. 5A). Similar α-synuclein aggregates morphologies were observed in post-mortem human brain of patients with PD (Raiss et al., 2016). The nuclear α-synuclein fraction has a higher tendency to aggregate compared to α-synuclein located in the cytoplasm (Lee et al., 2005). LC-like substances in the environment and pesticides have long been suspected to induce PD; therefore, gene-environment interactions could potentially shape the development and onset of the disease. Treatment with U-133 prevented and reversed the formation of α-synuclein

aggregates, as observed by confocal microscopy (Fig. 5A) and Filter Trap Assay (Fig. 5B and C). Further, HSP70 was found to be co-localized with α-synuclein mostly in damaged cells (Fig. 5D). The elevation of HSP70 in mouse α-synuclein overexpression models and human cell culture has recently been demonstrated to reduce α-synuclein aggregation (Klucken et al., 2004). Moreover, the disaggregase complex consisting of HSP70, the class B J-protein DNAJB1, and an HSP110 family nucleotide exchange factor, provides ATP-dependent activity that disassembles α-synuclein amyloid within minutes, via combined fibril fragmentation and depolymerization (Gao et al., 2015; McLean et al., 2004); our findings show similar effects of the HSP70 inducer.

An important hallmark of pathological PD is neuroinflammation (i.e. microglia activation and lymphocyte infiltration) provoked by the release of misfolded α-synuclein from damaged neurons (Béraud et al., 2013). In vivo imaging and *postmortem* immunohistochemical studies have established that PD is associated with an increase in the number of different microglial phenotypes, and the presence of proinflammatory mediators in the SNpc (Ouchi et al., 2009; Gerhard et al., 2006).

In the clinical PD stage induced by LC, we observed an elevation of Iba-1 positive cells, suggesting an increase in the number of cells with a microglial phenotype. Treatment with U-133 decreased the amount of Iba1-positive cells, suggesting a reduction of microglial activation in the SNpc and diminished neuroinflammation (Fig. 5E and F).

The results of this study demonstrate that a decline in HSP70 expression increases the vulnerability of nigral DA neurons to LC cytotoxicity in rats, and this might be a predisposing factor for the onset and progression of PD. Here, we present evidence that HSP70 over-expression, via U-133 HSP70 inducer, in DA neurons of the SNpc protects the animals from LC-induced PD-like symptoms. We show that the treated animals display improved DA neuronal health, better locomotor performance, and reduced motor disturbances. LC-induced disturbances, like α-synuclein aggregation and microglia activation, were greatly reversed upon HSP70 administration. Taken together, our findings strongly support the neuroprotective potential of exogenous HSP70 and the U-133 HSP70 inducer for the prevention and/or diminution of PD-like neurodegeneration. In conclusion, we have presented a robust method of protection against LC-induced PD-like symptoms in rodents using a key molecular chaperone.

5. Conclusion

We report here the first successful treatment of Parkinson's-like symptoms in a rodent model of the disease using a novel synthetic small molecule activator of HSP70 synthesis. These results provide evidence that the administration of the pro-drug may have considerable therapeutic potential for the protection of neurons involved in Parkinson's disease pathology. The novel compound may be employed for the therapy of a number of proteotoxic diseases besides Parkinson's disease, including Alzheimer's disease, Amyotrophic lateral sclerosis, and others, for which no effective treatments currently exist.

Acknowlegements

Competing interests

The authors declare that they have no competing interests.

Appendix A. Supplementary data

Supplementary data to this article can be found online at https://doi.org/10.1016/j.expneurol.2018.04.012.

References

Ahn, T.B., Jeon, B.S., 2006. Protective role of heat shock and heat shock protein 70 in lactacystin-induced cell death both in the rat substantia nigra and PC12 cells. Brain Res. 1087, 159–167. http://dx.doi.org/10.1016/j.brainres.2006.02.097.

Ascherio, A., Schwarzschild, M.A., 2016. The epidemiology of Parkinson's disease: risk factors and prevention. Lancet Neurol. 15, 1257–1272. http://dx.doi.org/10.1016/S1474-4422(16)30230-7.

Auluck, P., Chan, H.Y., Trojanowski, J.Q., Lee, V.M., Bonini, N.M., 2002. Chaperone suppression of α-synuclein toxicity in a Drosophila model for Parkinson's disease. Science 295, 865–868. http://dx.doi.org/10.1126/science.1067389.

Balchin, D., Hayer-Hartl, M., Hartl, F.U., 2016. In vivo aspects of protein folding and quality control. Science 353 aac4354-1–aac4354-12. https://doi.org/10.1126/science.aac4354.

Bao, X.Q., Wang, X.L., Zhang, D., 2017. FLZ Attenuates α-synuclein-induced neurotoxicity by activating heat shock protein 70. Mol. Neurobiol. 54, 349–361 (doi:71007/s12035-015-9572-9).

Bentea, E., Verbruggen, L., Massie, A., 2017. The proteasome inhibition model of Parkinson's disease. J Park. Dis. 7, 31–63.

Béraud, D., Hathaway, H.A., Trecki, J., Chasovskikh, S., Johnson, D.A., Federoff, H.J., et al., 2013. Microglial activation and antioxidant responses induced by the Parkinson's disease protein α-synuclein. J. NeuroImmune Pharmacol. 8, 94–117. http://dx.doi.org/10.1007/s11481-012-9401-0.

Bezard, E., Dovero, S., Prunier, C., Ravenscroft, P., Chalon, S., Guilloteau, D., et al., 2001. Relationship between the appearance of symptoms and the level of nigrostriatal degeneration in a progressive 1-methyl-4-phenyl-1,2,3,6-tetrahydropyridine-lesioned macaque model of Parkinson's disease. J. Neurosci. 21, 6853–6861.

Bobkova, N.V., Garbuz, D.G., Nesterova, I., Medvinskaya, N., Samokhin, A., Alexandrova, et al., 2014. Therapeutic effect of exogenous HSP70 in mouse models of Alzheimer's disease. J. Alzheimers Dis. 38, 425–435. http://dx.doi.org/10.3233/JAD-130779.

Braak, H., Del Tredici, K., Rüb, U., De Vos, R.A., Jansen Steur, E.N., Braak, E., 2003. Staging of brain pathology related to sporadic Parkinson's disease. Neurobiol. Aging 24, 197–211.

Bukhatwa, S., Zeng, B.Y., Rose, S., Jenner, P., 2010. A comparison of changes in proteasomal subunit expression in the substantia nigra in Parkinson's disease, multiple system atrophy and progressive supranuclear palsy. Brain Res. 1326, 174–183.

Chu, Y., Dodiya, H., Aebischer, P., Olanow, C.W., Kordower, J.H., 2009. Alterations in lysosomal and proteasomal markers in Parkinson's disease: relationship to alpha-synuclein inclusions. Neurobiol. Dis. 35, 385–398. http://dx.doi.org/10.1016/j.nbd.2009.05.023.

Ciechanover, A., Kwon, Y.T., 2015. Degradation of misfolded proteins in neurodegenerative diseases: therapeutic targets and strategies. Exp. Mol. Med. 47, e147. http://dx.doi.org/10.1038/emm.2014.117.

Das, C., Hoang, Q.Q., Kreinbring, C.A., Luchansky, S.J., Meray, R.K., Ray, S.S., et al., 2006. Structural basis for conformational plasticity of the Parkinson's disease-associated ubiquitin hydrolase UCH-L1. Proc. Natl. Acad. Sci. U. S. A. 103, 4675–4680.

Davie, C.A., 2008. A review of Parkinson's disease. Br. Med. Bull. 86, 109–127. http://dx.doi.org/10.1093/bmb/ldn013.

De Lau, L.M., Breteler, M.M., 2006. Epidemiology of Parkinson's disease. Lancet Neurol. 5, 525–535. http://dx.doi.org/10.1016/S1474-4422(06)70471-479.

Dong, Z., Wolfer, D.P., Lipp, H.P., Büeler, H., 2005. Hsp70 gene transfer by adeno-associated virus inhibits MPTP-induced nigrostriatal degeneration in the mouse model of Parkinson's disease. Mol. Ther. 11, 80–88. http://dx.doi.org/10.1016/j.ymthe.2004.09.007.

Dorsey, E.R., Constantinescu, R., Thompson, J.P., Biglan, K.M., Holloway, R.G., Kieburtz, K., et al., 2007. Projected number of people with Parkinson disease in the most populous nations, 2005 through 2030. Neurology 68, 384–386. http://dx.doi.org/10.1212/01.wnl.0000247740.47667.03.

Ebrahimi-Fakhari, D., Wahlster, L., McLean, P.J., 2011. Molecular chaperones in Parkinson's disease – present and future. J. Park. Dis 1, 299–320.

Ekimova, I.V., Nitsinskaya, L.E., Romanova, I.V., Pastukhov, Y.F., Margulis, B.A., Guzhova, I.V., 2010. Exogenous protein HSP70/Hsc70 can penetrate into brain structures and attenuate the severity of chemically-induced seizures. J. Neurochem. 115, 1035–1044. http://dx.doi.org/10.1111/j.1471-4159.2010.06989.x.

Gao, X., Carroni, M., Nussbaum-Krammer, C., Mogk, A., Nillegoda, N.B., Szlachcic, A., et al., 2015. Human Hsp70 disaggregase reverses Parkinson's-linked α-synuclein amyloid fibrils. Mol. Cell 59, 781–793. http://dx.doi.org/10.1016/j.molcel.2015.07.012.

Gerhard, A., Pavese, N., Hotton, G., Turkheimer, F., Es, M., Hammers, A., et al., 2006. In vivo imaging of microglial activation with [11C](R)-PK11195 PET in idiopathic Parkinson's disease. Neurobiol. Dis. 21, 404–412. http://dx.doi.org/10.1016/j.nbd.2005.08.002.

Gomez, C., Santiago-Mejia, J., Ventura-Martinez, R., Rodriguez, R., 2006. The sunflower

seed test: a simple procedure to evaluate forelimb motor dysfunction after brain ischemia. Drug Dev. Res. 67, 752–756.

Hartl, F.U., Bracher, A., Hayer-Hartl, M., 2011. Molecular chaperones in protein folding and proteostasis. Nature 475, 324–332. http://dx.doi.org/10.1038/nature10317.

Hightower, L.E., Guidon Jr., P.T., 1989. Selective release from cultured mammalian cells of heat-shock (stress) proteins that resemble glia-axon transfer proteins. J. Cell. Physiol. 138, 257–266. http://dx.doi.org/10.1002/jcp.1041380206.

Jung, A.E., Fitzsimons, H.L., Bland, R.J., During, M.J., Young, D., 2008. HSP70 and constitutively active HSF1 mediate protection against CDCrel-1-mediated toxicity. Mol. Ther. 16, 1048–1055. http://dx.doi.org/10.1038/mt.2008.68.

Kalmar, B., Lu, C.H., Greensmith, L., 2014. The role of heat shock proteins in Amyotrophic Lateral Sclerosis: the therapeutic potential of Arimoclomol. Pharmacol. Ther. 141, 40–54. http://dx.doi.org/10.1016/j.pharmthera.2013.08.003.

Kalueff, A.V., Keisala, T., Minasyan, A., Kumar, S.R., LaPorte, J.L., Murphy, D.L., et al., 2008. The regular and light–dark Suok tests of anxiety and sensorimotor integration: utility for behavioral characterization in laboratory rodents. Nat. Protoc. 3, 129–136. http://dx.doi.org/10.1038/nprot.2007.516.

Kane, J.R., Ciucci, M.R., Jacobs, A.N., Tews, N., Russell, J.A., Ahrens, A.M., et al., 2011. Assessing the role of dopamine in limb and cranial-oromotor control in a rat model of Parkinson's disease. J. Commun. Disord. 44, 529–537. http://dx.doi.org/10.1016/j.jcomdis.2011.04.005.

Kim, S., Nollen, E.A., Kitagawa, K., Bindokas, V.P., Morimoto, R.I., 2002. Polyglutamine protein aggregates are dynamic. Nat. Cell Biol. 4, 826–831. http://dx.doi.org/10.1038/ncb863.

Kisselev, A.F., Goldberg, A.L., 2001. Proteasome inhibitors: from research tools to drug candidates. Chem. Biol. 8, 739–758.

Klucken, J., Shin, Y., Hyman, B.T., McLean, P.J., 2004. A single amino acid substitution differentiates HSP70-dependent effects on α-synuclein degradation and toxicity. Biochem. Biophys. Res. Commun. 325, 367–373. http://dx.doi.org/10.1016/j.bbrc.2004.10.037.

Konieczny, J., Jantas, D., Lenda, T., Domin, H., Czarnecka, A., Kuter, K., et al., 2014. Lack of neuroprotective effect of celastrol under conditions of proteasome inhibition by lactacystin in in vitro and in vivo studies: implications for Parkinson's disease. Neurotox. Res. 26, 255–273. http://dx.doi.org/10.1007/s12640-014-9477-9.

Labbadia, J., Morimoto, R.I., 2015. The biology of proteostasis in aging and disease. Annu. Rev. Biochem. 84, 435–464. http://dx.doi.org/10.1146/annurev-biochem-060614-033955.

Lasunskaia, E.B., Fridlianskaia, I., Arnholdt, A.V., Kanashiro, M., Guzhova, I., Margulis, B.A., 2010. Sub-lethal heat shock induces plasma membrane translocation of 70-kDa heat.shock protein in viable, but not in apoptotic, U-937 leukaemia cells. APMIS 118, 179–187. http://dx.doi.org/10.1111/j.1600-0463.2009.02576.x.

Lazarev, V.F., Onokhin, K.V., Antimonova, O.I., Polonik, S.G., Guzhova, I.V., Margulis, B.A., 2011. Kinetics of chaperone activity of proteins HSP70 and Hdj1 in human leukemia U-937 cells after preconditioning with thermal shock or compound U-133. Biochem. Mosc. 76, 590–595. http://dx.doi.org/10.1134/S0006297911050099.

Lazarev, V.F., Nikotina, A.D., Mikhaylova, E.R., Nudler, E., Polonik, S.G., Guzhova, I.V., et al., 2016. Hsp70 chaperone rescues C6 rat glioblastoma cells from oxidative stress by sequestration of aggregating GAPDH. Biochem. Biophys. Res. Commun. 470, 766–771. http://dx.doi.org/10.1016/j.bbrc.2015.

Lazarev, V.F., Mikhaylova, E.R., Guzhova, I.V., MArgulis, B.A., 2017. Possible function of molecular chaperones in diseases caused by propagating amyloid aggregates. Front. Neurosci. 16 (11), 277. http://dx.doi.org/10.1134/S0006297911050099.

Lee, H.J., Patel, S., Lee, S.J., 2005. Intravesicular localization and exocytosis of alpha-synuclein and its aggregates. J. Neurosci. 25, 6016–6024. http://dx.doi.org/10.1523/JNEUROSCI.0692-05.2005.

McLean, P.J., Klucken, J., Shin, Y., Hyman, B.T., 2004. Geldanamycin induces HSP70 and prevents α-synuclein aggregation and toxicity in vitro. Biochem. Biophys. Res. Commun. 321, 665–669. http://dx.doi.org/10.1016/j.bbrc.2004.07.021.

McNaught, K.S., Björklund, L.M., Belizaire, R., Isacson, O., Jenner, P., Olanow, C.W., 2002. Proteasome inhibition causes nigral degeneration with inclusion bodies in rats. NeuroReport 13, 1437–1441.

McNaught, K.S., Perl, D.P., Brownell, A.L., Olanow, C.W., 2004. Systemic exposure to

proteasome inhibitors causes a progressive model of Parkinson's disease. Ann. Neurol. 56, 149–162. http://dx.doi.org/10.1002/ana.20186.

Mendillo, M.L., Santagata, S., Koeva, M., Bell, G.W., Hu, R., Tamimi, R.M., Fraenkel, E., Ince, T.A., Whitesell, L., Lindquist, S., 2012. HSF1 drives a transcriptional program distinct from heat shock to support highly malignant human cancers. Cell 150, 549–562.

Mingozzi, F., High, K., 2011. Immune responses to AAV in clinical trials. Curr. Gene Ther. 11, 321–330.

Mittoux, V., Ouary, S., Monville, C., Lisovoski, F., Poyot, T., Conde, F., et al., 2002. Corticostriatopallidal neuroprotection by adenovirus-mediated ciliary neurotrophic factor gene transfer in a rat model of progressive striatal degeneration. J. Neurosci. 22, 4478–4486(DOI: 20026446).

Ouchi, Y., Yagi, S., Yokokura, M., Sakamoto, M., 2009. Neuroinflammation in the living brain of Parkinson's disease. Parkinsonism Relat. Disord. 15, S200–S204.

Paxinos, G., Watson, C., 1986. The Rat Brain in Stereotaxic Coordinates. CA Acad, San Diego.

Raiss, C.C., Braun, T.S., Konings, I.B., Grabmayr, H., Hassink, G.C., Sidhu, A., et al., 2016. Functionally different α-synuclein inclusions yield insight into Parkinson's disease pathology. Sci. Rep. 6, 23116. http://dx.doi.org/10.1038/srep23116.

Riederer, P., Wuketich, S., 1976. Time course of nigrostriatal degeneration in Parkinson's disease. J. Neural Transm. 38, 277–301.

Roberts, H.L., Brown, D.R., 2015. Seeking a mechanism for the toxicity of oligomeric α-synuclein. Biomol. Ther. 5, 282–305. http://dx.doi.org/10.3390/biom5020282.

Rodríguez-Nogales, C., Garbayo, E., Carmona-Abellán, M.M., Luquin, M.R., Blanco-Prieto, M.J., 2016. Brain aging and Parkinson's disease: new therapeutic approaches using drug delivery systems. Maturitas 84, 25–31. http://dx.doi.org/10.1016/j.maturitas.2015.

Salganik, M., Sergeyev, V.G., Shinde, V., Meyers, C.A., Gorbatyuk, M.S., Lin, J.H., et al., 2015. The loss of glucose-regulated protein 78 (GRP78) during normal aging or from siRNA knockdown augments human alpha-synuclein (α-syn) toxicity to rat nigral neurons. Neurobiol. Aging 36, 2213–2223. http://dx.doi.org/10.1016/j.neurobiolaging.2015.02.018.

Shimura, H., Schlossmacher, M.G., Hattori, N., Frosch, M.P., Trockenbacher, A., Schneider, R., 2001. Ubiquitination of a new form of alpha-synuclein by parkin from human brain: implications for Parkinson's disease. Science 293, 263–269.

Singleton, A.B., Farrer, M., Johnson, J., Singleton, A., Hague, S., Kachergus, J., et al., 2003. Alfa-Synuclein locus triplication causes Parkinson's disease. Science 302, 841. http://dx.doi.org/10.1126/science.1090278.

Smith, S.L., Thompson, K.S., Sargent, B.J., Heal, D.J., 2001. BTS 72664 - a novel CNS drug with potential anticonvulsant, neuroprotective, and antimigraine properties. CNS Drug Rev. 7, 146–171.

Taylor, C.R., Levenson, R.M., 2006. Quantification of immunohistochemistry tissues concerning methods, utility and semiquantitative assessment II. Histopathology 49, 411–424. http://dx.doi.org/10.1111/j.1365-2559.2006.02513.x.

Tillerson, J.L., Caudle, W.M., Reveron, M.E., Miller, G.W., 2002. Detection of behavioral impairments correlated to neurochemical deficits in mice treated with moderate doses of 1-methyl-4-phenyl-1,2,3,6-tetrahydropyridine. Exp. Neurol. 178, 80–90.

Tolleson, C.M., Fang, J.Y., 2013. Advances in the mechanisms of Parkinson's disease. Discov. Med. 15, 61–66.

Tydlacka, S., Wang, C.E., Wang, X., Li, S., Li, X.J., 2008. Differential activities of the ubiquitin-proteasome system in neurons versus glia may account for the preferential accumulation of misfolded proteins in neurons. J. Neurosci. 28, 13285–13295. http://dx.doi.org/10.1523/JNEUROSCI.4393-08.2008.

Tytell, M., Greenberg, S.G., Lasek, R.J., 1986. Heat shock-like protein is transferred from.glia to axon. Brain Res. 363, 161–164.

Westerheide, S.D., Bosman, J.D., Mbadugha, B.N., Kawahara, T.L., Matsumoto, G., Kim, S., et al., 2004. Celastrols as inducers of the heat shock response and cytoprotection. J. Biol. Chem. 279, 56053–56060. http://dx.doi.org/10.1074/jbc.M409432200.

Yurchenko, E.A., Menchinskaya, E.S., Polonik, S.G., Agafonova, I.G., Guzhova, I.V., Margilis, B.A., Aminin, D.L., 2015. Hsp70 induction and anticancer activity of U-133, the acytilated trisglucosydic derivative of echinochrome. Med. Chem. 5 (6). http://dx.doi.org/10.4172/2161-0444.1000274.